

Structural, electronic and vibrational properties of indium oxide clusters

This article has been downloaded from IOPscience. Please scroll down to see the full text article.

2011 Chinese Phys. B 20 063101

(<http://iopscience.iop.org/1674-1056/20/6/063101>)

View [the table of contents for this issue](#), or go to the [journal homepage](#) for more

Download details:

IP Address: 202.120.52.109

The article was downloaded on 12/06/2011 at 16:57

Please note that [terms and conditions apply](#).

Structural, electronic and vibrational properties of indium oxide clusters

Xu Mao-Jie(徐茂杰)^{a)}, Ni Yi(倪一)^{b)}, Li Zhen-Qing(李振庆)^{a)}, Wang Sheng-Li(王胜利)^{a)},
Liu Xiao-Hui(柳效辉)^{a)}, and Dou Xiao-Ming(窦晓鸣)^{b)a)c)†}

^{a)}Department of Physics, Shanghai Jiao Tong University, Shanghai 200240, China

^{b)}School of Optical-electrical and Computer Engineering, University of Shanghai for Science and Technology, Shanghai 200093, China

^{c)}Consolidated Research Institute for Advanced Science and Medical Care, Waseda University, Tokyo 162-0041, Japan

(Received 9 August 2010; revised manuscript received 6 January 2011)

Geometric, electronic and vibrational properties of the most stable and energetically favourable configurations of indium oxide clusters In_mO_n ($1 \leq m, n \leq 4$) are investigated using density functional theory. The lowest energy geometries prefer the planar arrangement of the constituent atoms with a trend to maximize the number of ionic In–O bonds. Due to the charge transfer from In to O atoms, the electrostatic repulsion occurs between the atoms with the same kind of charge. The minimization of electrostatic repulsion and the maximization of In–O bond number compete between each other and determine the location of the isometric total energy. The most stable linear In–O–In–O structure of In_2O_2 cluster is attributed to the reduced electrostatic repulsive energy at the expense of In–O bond number, while the lowest energy rhombus-like structure of In_2O_3 cluster reflects the maximized number of In–O bonds. Furthermore, the vibrational frequencies of the lowest energy clusters are calculated and compared with the available experimental results. The energy gap and the charge density distribution for clusters with varying oxygen/indium ratio are also discussed.

Keywords: indium oxide cluster, equilibrium structure, vibrational frequency

PACS: 31.15.ae, 31.15.eg

DOI: 10.1088/1674-1056/20/6/063101

1. Introduction

Indium oxide (In_2O_3) has aroused the considerable interest for the multiple applications in microelectronics and optoelectronics. It exhibits a wide band gap^[1–3] and is a suitable candidate for the fabrication of various devices such as field-effect transistors, light-emitting diodes, barrier layer in tunnel junctions and solar cells.^[4–6] Tin-doped indium oxides are well known as transparent conducting oxides (TCOs) widely used in a range of devices such as liquid crystal displays and solar panels.^[7–12] Many efforts have been made to understand structural, optical and electronic properties of indium oxide. Its basic optoelectronic and surface electronic properties are still under intense debate. In recent years, the properties and the applications of indium oxide nanostructures have been extensively studied. The very high surface-to-volume ratio can facilitate new and novel applications of indium oxide. An outstanding example is the use of indium oxide nanowire as chemical gas sensor,^[13]

which is expected to increase the gas-sensing reaction time and reduce the power requirement.

Small clusters of indium oxide provide the prototype model to understand the physics and chemistry of the formed nanostructures. There are experimental observations and theoretical calculations of equilibrium structures, vibrations and electronic properties of indium oxide clusters.^[14–18] The experimental studies using matrix isolation technique and infrared (IR) absorption spectroscopy reported that the In_2O_2 and In_2O_3 clusters have the symmetric linear In–O–In–O and In–O–In–O–In structures.^[15] The band observed at 816.6 cm^{-1} is assigned to the linear In–O–In–O and 826.6 cm^{-1} assigned to the linear In–O–In–O–In. Density functional theory and *ab initio* studies appeared to establish the linear structures as the global minima on the potential energy surface.^[16,17] Previous IR spectrum study also implied that the band at 609.0 cm^{-1} was assigned to In_mO_n for $m, n \geq 2$,^[15] which invokes the theoretical work for a further understanding of structural, electronic and vi-

[†]Corresponding author. E-mail: xmdou@sjtu.edu.cn

brational properties of these clusters.

In the present work, the lowest energy and energetically favorable configurations of In_mO_n clusters for $1 \leq m, n \leq 4$ are explored using density functional theory at B3LYP level. The computed results are presented on the equilibrium structures, electronic states and vibrational properties of these clusters. The predicted vibrational frequencies and bands are compared with the available experimental results.

2. Computational method

The geometrical optimization and the electronic structure calculation were conducted in the framework of density-functional theory (DFT) through Becke's three-parameter hybrid functional and Lee–Yang–Parr correlation functional (B3LYP)^[19,20] with 6-31G(D) basis set for oxygen atom and LanL2DZ for indium atom, respectively. The isomers analysed in this study are fully optimized with the convergence criteria for an energy of 10^{-6} Hartree (1 Hartree = 27.21 eV). The vibrational frequencies of the lowest energy configurations are computed under harmonic approximation with the analytical force constants. All the calculations are performed by GAUSSIAN 03 codes.^[21]

The reliability of the DFT–B3LYP approach was demonstrated in the previous theoretical investigation on the structures and vibrations of $M_2\text{O}_2$ clusters ($M = \text{Al}, \text{Ga}, \text{In}, \text{Tl}$).^[16] The predicted harmonic vibrational frequencies accord well with the available experimental data. Therefore, B3LYP method is applicable for theoretical study of indium oxide clusters.

3. Results and discussion

Several linear, planar and nonplanar configurations of indium oxide clusters are dealt with through DFT calculations. Some configurations are initialized by considering previously reported structures of gallium oxide clusters.^[22–25] Figure 1 shows the lowest energy and energetically favorable configurations of indium oxide clusters. All the lowest energy structures exhibit low spin electronic state with the exception of In_2O_3 cluster, which has spin triplet electronic state. The corresponding total energy, symmetry, interatomic distance and the energy difference of various

isomers are collected in Table 1. In the following subsections, the equilibrium structures, vibrational properties and electronic stabilities of these clusters are discussed.

3.1. Equilibrium structures

(i) In_3O

Figure 1(1a) shows the lowest energy configuration of In_3O , a T-type C_{2v} structure with spin doublet electronic state. It has the base $R_{\text{In-O}}$ of 2.04 Å (1 Å = 0.1 nm) and the apex $R_{\text{In-O}}$ of 2.22 Å. The In_3O isomers prefer to bond the extra In atom directly to the O atom, which increases the number of In–O bonds. The optimization of the hyper-metallic In_3O structure with In_3 cluster is converged to the lowest T-type configuration. The formation of metallic In–In bond is found to be energetically unfavorable and the formation of the third additional In–O bond is expected to lower the total energy monotonically during the convergence from the hyper-metallic structure to T-type one. The computed results do not show the stable D_{3h} isomer. The Jahn–Teller distortion is expected to lower its energy and lead to the T or Y type geometry. The next low lying isomer is the $C_{\infty v}$ linear structure at 0.66 eV above (see Fig. 1(1b)).

(ii) In_3O_2

The lowest energy configuration of In_3O_2 is found to be a doublet planar rhombus-like configuration with the extra oxygen attached to one In atom (see Fig. 1(2a)). The next isomer is a planar V-shape C_{2v} configuration at 0.32 eV above, which is obtained from the optimization of a closed-pentagonal ring. Figure 1(2c) shows a Y-shape configuration following in the higher energy at 2.34 eV.

(iii) In_4O_3

The calculated lowest energy configuration is a singlet planar Y-shape C_{2v} structure, as shown in Fig. 1(3a). It can be viewed as three terminal O–In units attached to one In atom. The next isomer is a rhombus-like configuration with two terminal In and one terminal O atoms at 1.51 eV higher in energy. A nonplanar triangular configuration follows at 1.83 eV (see Fig. 1(3c)). It is composed of two triangles, one is for O atoms and the other is for In atoms on its top, with the fourth oxygen above the In triangle. The next low lying structure is a rhombus-like configuration with one terminal In and one terminal In–O unit at 2.10 eV higher in the energy.

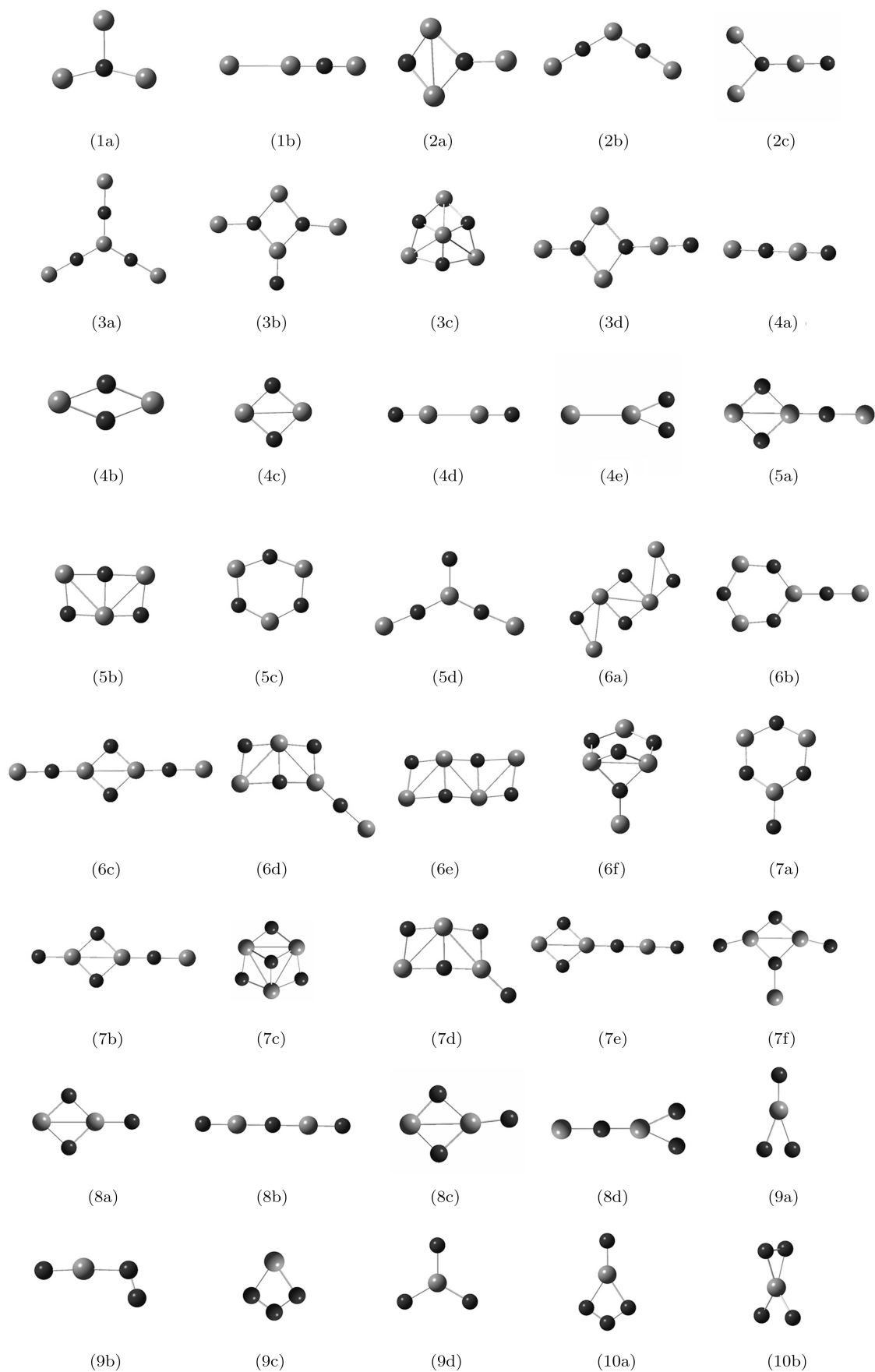


Fig. 1. The lowest energy and energetically favorable configurations of indium oxide clusters. The grey solid circles represent indium atoms and the black solid circles denote oxygen atoms.

Table 1. Total energy (Hartree), symmetry and interatomic distance (Å) of the most stable and the low lying geometries of indium oxide clusters, and the energy difference ΔE (eV) between the lowest energy and low lying structures.

	E	sym.	$R_{\text{In-In}}$	$R_{\text{O-O}}$	$R_{\text{In-O}}$	ΔE
In ₃ O						
(1a)	-80.9798075	C_{2v}	3.35		2.04, 2.22	0.0
(1b)	-80.9553814	$C_{\infty v}$				0.66
In ₃ O ₂						
(2a)	-156.2565966	C_{2v}	3.08	2.73	1.95, 1.98, 2.17	0.0
(2b)	-156.2448089	C_{2v}				0.32
(2c)	-156.1706157	C_s				2.34
In ₄ O ₃						
(3a)	-233.4692672	C_{3v}	3.81	3.29	1.90, 1.91	0.0
(3b)	-233.4139164	C_{2v}				1.51
(3c)	-233.4021374	C_{3v}				1.83
(3d)	-233.3919331	C_s				2.10
In ₂ O ₂						
(4a)	-154.2917953	$C_{\infty v}$	3.79	3.62	1.77, 1.85, 1.95	0.0
(4b)	-154.2571486	D_{2h}				0.94
(4c)	-154.2454004	D_{2h}				1.26
(4d)	-154.1954007	$C_{\infty v}$				2.62
(4e)	-154.1565993	C_{2v}				3.68
In ₃ O ₃						
(5a)	-231.5010482	C_{2v}	2.85	2.74	1.87, 1.93, 1.96, 1.98	0.0
(5b)	-231.4972997	C_{2v}				0.10
(5c)	-231.4808683	C_{2v}				0.55
(5d)	-231.4763868	C_{2v}				0.67
In ₄ O ₄						
(6a)	-308.7124037	C_{2h}	2.93	2.78	1.85, 1.90, 2.13, 2.37	0.0
(6b)	-308.7050239	C_{2v}				0.20
(6c)	-308.6829676	C_{2h}				0.80
(6d)	-308.6719818	C_s				1.10
(6e)	-308.6574685	C_s				1.49
(6f)	-308.6238562	C_1				2.41
In ₃ O ₄						
(7a)	-306.6822035	C_{2v}	3.43	3.19	1.91, 1.93	0.0
(7b)	-306.6535737	C_{2v}				0.79
(7c)	-306.6399776	C_{3v}				1.15
(7d)	-306.6396905	C_s				1.16
(7e)	-306.6236409	C_{2v}				1.59
(7f)	-306.6105186	C_{2v}				1.95
In ₂ O ₃						
(8a)	-229.4735869	C_{2v}	2.83	2.73	1.94, 1.95, 1.99	0.0
(8b)	-229.4733431	$C_{\infty v}$				0.01
(8c)	-229.4386369	C_s				0.95
(8d)	-229.4098645	C_s				1.73
InO ₃						
(9a)	-227.3937561	C_{2v}		1.44	1.81, 2.13	0.0
(9b)	-227.3931214	C_s				0.02
(9c)	-227.3749024	C_{2v}				0.51
(9d)	-227.3404583	D_{3h}				1.45
InO ₄						
(10a)	-302.6508479	C_{2v}		1.37	1.79, 2.07	0.0
(10b)	-302.6035276	C_{2v}				1.29

(iv) In_2O_2

Different isomeric configurations of In_2O_2 cluster are considered, as shown in Figs. 1(4a)–1(4e). The total energy calculations for all isomers are performed in singlet and triplet electronic states. The singlet states are found to be lower in energy than the triplet ones. The most stable isomer exhibits the linear In–O–In–O configuration. From the viewpoint of bond energetics, the D_{2h} rhombus structure with 42.5° O–In–O bond angle and 1.56 Å O–O separation is composed of the higher number of In–O bonds than the lowest linear structure. However, due to the charge transfer between In and O atoms, there is the strong electrostatic repulsion between likely charged atoms in the D_{2h} isomer. The electrostatic repulsion competes with the number of In–O bonds and results in the D_{2h} isomer at 0.94 eV higher in energy than the lowest linear configuration. The next low lying isomer is the D_{2h} isometric structure with the bond angle close to 90° . It is 1.26 eV above in energy. The electrostatic repulsion is stronger for this isomer as a result of larger charge transfer (0.85 e), as compared with the former D_{2h} isomer (0.58 e). Figure 1(4d) exhibits the $D_{\infty h}$ O–In–In–O isomer following at 2.62 eV in energy. The next low lying configuration is a Y-shape C_{2v} structure. This isomer forms the energetically unfavorable In–In bond and is located at a much higher energy, 3.67 eV.

(v) In_3O_3

Figure 1(5a) shows the lowest energy geometry of In_3O_3 , a rhombus-like C_s structure in spin doublet electronic state. A planar window-pane C_{2v} structure is found to be almost degenerate with the most stable structure, 0.10 eV above in energy (see Fig. 1(5b)). The next low lying configuration is a planar hexagonal cyclic structure with alternating In–O sequence at 0.55 eV. A Y-shape C_s structure is located at 0.67 eV. The stability of In_3O_3 isomer is slightly different from that of Ga_3O_3 . The most stable geometry of Ga_3O_3 is the planar window-pane C_{2v} structure. The maximization of the coordination number for Ga atoms is found to play a central role in stabilizing the gallium oxide cluster.^[22] In the case of In_3O_3 , it is energetically favourable to have the coordination number of 2 for the O atoms even though the coordination number is 1 for In atoms. The coordination numbers of In atoms in the most stable rhombus-like C_s structure are 3, 2 and 1 and those of O atoms are all 2, whereas the planar window-pane C_{2v} structure has the coordi-

nation number of 3 for the inner In and O atoms and the coordinate number of 2 for the outside In and O atoms.

(vi) In_4O_4

Figure 1(6a) displays a di-bridge rhombus configuration with singlet electronic state, in which two terminal In–O units are bent by an angle of 136.7° . A hexagonal ring configuration with one terminal O–In unit follows at 0.20 eV above in energy. The next isomer is also a di-bridge rhombus configuration in which two terminal In–O units are attached to two rhombus In atoms and the In–O–In terminal units are linear (see Fig. 1(6c)). The next low lying structures are a window-pane configuration with a terminal In–O unit attached to one outside In atom and a compact window-pane configuration with no terminal. A non-planar distorted hexagonal ring configuration with a terminal O–In unit attached to two In atoms follows at 2.41 eV above (see Fig. 1(6d)).

(vii) In_3O_4

The lowest energy configuration comes out to be a doublet planar C_{2v} hexagonal ring configuration with a terminal O atom attached to an In atom. The next isomer is a rhombus-like structure with terminal O atom and O–In unit. Figure 1(7c) shows a nonplanar C_{3v} isomer following at 1.15 eV above in energy. In this configuration, one In equilateral triangle forms above one equilateral triangle of O atoms with the fourth oxygen on the top of In triangle. Alternatively, it can be considered as an oxygen tetrahedron intercepted by an indium triangle. The next low lying structure is a planar window-pane configuration with a terminal O atom. It is followed by a rhombus-like configuration with one terminal O–In–O unit and a rhombus-like structure with one terminal In and two terminal O atoms.

(viii) In_2O_3

The most stable geometry of In_2O_3 is the rhombus-like C_{2v} configuration in triplet electronic state (see Fig. 1(8a)), which can be considered as an extension of a rhombus In_2O_2 configuration with an O atom attached to one of the In atom. The energy difference of triplet-singlet state is high (0.95 eV). The next isomer of a linear structure is almost degenerate in energy, only 0.01 eV above. Figure 1(8d) is a Y-shape structure located in higher energy, 1.73 eV above.

(ix) InO_3

Figure 1(9a) shows a Y-type structure in spin doublet electronic state with a terminal In–O bond of 1.81 Å and an inner In–O bond of 2.13 Å. The planar L-type C_s structure is almost degenerate with the doublet Y-type isomer, only 0.02 eV higher in energy. A planar distorted rhombus isomer is located at 0.93 eV above. A quartet D_{3h} isomeric configuration follows at 1.87 eV.

(x) InO_4

The lowest energy structure of InO_4 cluster has an O_3 cluster structure in doublet electronic state (see Fig. 1(10a)). The geometry of InO_4 is much different from that reported for the AlO_4 molecule.^[26,27] The lowest energy configuration of AlO_4 exhibits D_{2d} symmetry. In the case of InO_4 , the D_{2d} symmetric structure is not related to a stationary point but to a saddle point, because the imaginary vibrational frequency is found to appear in the vibrational spectrum. This means the D_{2d} structure does not yield an energy minimum on the potential energy surface. The next low lying isomer is a nonplanar C_{2v} configuration with one O–O distance of 1.37 Å and the other O–O distance of 2.37 Å.

3.2. Vibrations and band assignments

The harmonic vibrational frequencies are computed to verify the stabilities of the optimized ge-

ometries. As the imaginary frequency is associated with the saddle point, the corresponding configuration is not related to global or local minimum on the potential energy surface. The computed vibrational frequencies of the most stable configurations are collected in Table 2.

The lowest energy In_3O isomer exhibits in total six vibrational modes. The lower two modes correspond to the in-plane bending movements of the apex and base In atom. The next one is the out-of-plane bending of O atom. It is followed by the stretching mode of all In atoms. The fifth one displays the symmetric stretching of O atom to the apex atom. The last one reflects the asymmetric stretching of O atom to the base In atoms.

The lowest energy In_3O_2 isomer displays nine modes. The first mode corresponds to the in-plane bending of the terminal In atom. It is followed by the movements of the terminal In atom with the O atoms. The fourth mode displays the out-of-plane bending of two O atoms. The next one is the in-plane bending of tricoordinated oxygen, followed by the in-plane bending of the dicoordinated In atoms and the dicoordinated oxygen. The seventh mode reflects the stretching movement of the dicoordinated oxygen. The last two modes are related to the stretching of two O atoms.

Table 2. Vibrational frequencies (cm^{-1}) of the most stable configurations of indium oxide clusters.

In_3O		In_3O_2		In_3O_3		In_4O_3		In_4O_4		In_3O_4		InO_4		In_2O_3		In_2O_2		InO_3	
ω_e		ω_e		ω_e		ω_e		ω_e		ω_e		ω_e		ω_e		ω_e		ω_e	
57	b2	48	a'	20	a'	19	b2	25	a''	61	b1	98	a'	90	a''	53	π	24	b2
70	a1	84	a''	25	a''	20	a1	49	a'	93	a2	111	a''	117	a'	53	π	98	b1
128	b1	140	a'	123	a''	30	b1	61	a'	99	a1	244	a'	224	a'	168	π	212	b2
165	a1	176	a''	150	a'	95	b2	113	a''	105	b1	264	a''	228	a''	168	π	405	a1
297	a1	179	a'	152	a'	111	b1	115	a''	111	b2	308	a'	431	a'	200	σ_g	709	a1
447	a2	185	a'	232	a''	113	a2	163	a''	118	b2	678	a'	478	a'	730	σ_g	1037	a1
		457	a'	264	a'	149	a1	164	a'	192	a1	751	a'	516	a'	211	σ_g		
		462	a'	439	a'	200	a1	165	a'	202	b1	935	a'	543	a'				
		609	a'	466	a'	201	b2	208	a'	365	a1	992	a'	596	a'				
				525	a'	224	b1	257	a''	394	b2								
				578	a'	260	b2	336	a'	414	a1								
				786	a'	261	a1	343	a'	537	a1								
						797	a1	381	a'	621	b2								
						797	b2	405	a'	685	a1								
						831	a1	579	a'	694	b2								
								593	a'										
								657	a'										
								670	a'										

In total, fifteen modes are reflected in the vibrations of the most stable In_4O_3 isomer. The six lower frequency modes are attributed to the bending and the torsion movements of In and O atoms. The first and the second ones are related to the in-plane bending movements of terminal In atoms. The third one is out-of-plane bending of terminal In atom. The next ones are the in-plane bending and out-of-plane bending of O atoms. The seventh mode is the stretching movements of terminal In atoms with the inner O atoms. The next five modes reflect the in-plane and the out-of-plane bending of O atoms. The last three modes display the asymmetric and the symmetric stretching movements of O atoms.

The lowest energy In_2O_2 isomer has seven vibrational modes. The lower four vibrational modes are associated with the bending movements of O atoms in the directions perpendicular to the linear structure. The fifth mode corresponds to the stretching of In atoms. The last two modes are the stretching movements of O atoms.

The lower two vibrational modes of In_3O_3 cluster are associated with the in-plane and the out-of-plane bending movements of terminal In atom. The third and the fourth one are the in-plane and the out-of-plane bending movements of terminal O atom. The next one is the stretching of terminal In and O atoms. It is followed by the out-of-plane bending of all O atoms. The seventh mode displays the stretching movements of In atoms, followed by asymmetric stretching of the rhombus O atoms. The next one is the in-plane bending and stretching of the rhombus O atoms. The next two modes reflect the stretching of the rhombus O atoms. The last one is the symmetric stretching of the terminal O atom.

Eighteen vibrational modes are found for the lowest energy In_4O_4 structure. The lower three modes correspond to the out-of-plane and the in-plane bending of terminal In atoms. The first one is the out-of-plane bending and the other two are the in-plane bending. The next three modes reflect the out-of-plane bending of terminal O and rhombus O atoms. The seventh and the eighth one display in-plane bending movements of terminal In and O atoms. It is followed by the in-plane bending of the rhombus In atoms and the out-of-plane bending of all O atoms. The remaining modes exhibit the stretching of O atoms. The 11th–14th ones indicate the stretching of O atoms in the direction along the terminal In–O unit. The 15th–18th ones are for the stretching of O

atoms in the direction perpendicular to the terminal In–O units.

Fifteen vibrational modes are found for the lowest energy In_3O_4 structure. The first mode is associated with the out-of-plane bending of O atoms. The second one is related to the torsion of two O atoms in the hexagonal ring which are attached to the tricoordinated In atom. The next one is related to in-plane bending movements of ring O atoms. The fourth one exhibits the out-of-plane bending of O atoms. It is followed by the in-plane bending mode of the terminal O atom. The next two modes are for the in-plane bending of O atoms and In atoms. The eighth one reflects the out-of-plane bending of O atoms. The next three modes correspond to in-plane symmetric and asymmetric bending of O atoms. The last four ones reflect the symmetric and the asymmetric stretching movements of terminal O atoms and inner O atoms of the hexagonal ring.

The most stable In_2O_3 configuration has nine vibrational modes in total. The lower two modes are related to the out-of-plane and the in-plane bending of terminal O atom. The next one displays the in-plane bending of In atoms. The fourth mode reflects the out-of-plane bending of O atoms. It is followed by the stretching mode of the rhombus O atoms. The last three ones correspond to the stretching movements of all O atoms.

The lowest energy InO_3 isomer displays six vibrational modes. The lower two modes are related to the in-plane and the out-of-plane bending of terminal O atom. The next two are the asymmetric and the symmetric stretching modes of two inner O atoms. The fifth one corresponds to the stretching of terminal O atom. The last one is the in-plane bending of two inner O atoms.

The most stable InO_4 configuration exhibits nine vibrational modes. The lower two modes are related to the in-plane and the out-of-plane bending of terminal O atom. The next one reflects the symmetric stretching mode of two distorted rhombus O atoms which are attached to the In atom. The fourth mode displays the out-of-plane bending of three rhombus O atoms. It is followed by the asymmetric stretching of two rhombus O atoms to the In atom. The next one is the stretching of terminal O atom. The seventh one corresponds to the in-plane bending of two rhombus atoms. The last two modes are the asymmetric and the symmetric stretching of the O atom which bonds to other two O atoms.

In the infrared studies of matrix-isolated In_xO_y species, 816.0 cm^{-1} and 826.0 cm^{-1} bands were assigned to the linear In-O-In-O and O-In-O-In-O structures, respectively.^[15] The previously computed harmonic vibrational frequencies were found to correlate well with the experiment and support the assignment of In_2O_3 system.^[16,17] In the present study, the calculated vibrational frequencies confirm the band assignment to the linear structure in the previous experimental investigation. The 826.0 cm^{-1} band corresponds to the computed 888.0 cm^{-1} band of the linear O-In-O-In-O isomer. This band is assigned to the stretching of O atoms. The 816.0 cm^{-1} band is related to the computed 811.0 cm^{-1} band of the linear O-In-O-In isomer. This band is also assigned to the stretching of O atoms. The computed 593.0 cm^{-1} and 657.0 cm^{-1} oxygen stretching modes of In_4O_4 cluster may account for the experimental 609.0 cm^{-1} band.

3.3. Electronic stability

The highest occupied molecular orbital (HOMO) and the lowest unoccupied molecular orbital (LUMO) are important parameters to characterize the electronic stabilities of small clusters. The Koopmans theory demonstrates that the HOMO energy level is associated with the cluster ability of losing its electrons, while the LUMO energy level equals to the electron affinity potential and reflects the cluster ability of obtaining the electrons. The HOMO–LUMO gap (E_{gap}) determines the energy required by an electron hopping from the occupied orbital to unoccupied orbital. A large E_{gap} means a higher energy required to perturb the electronic structure. The small cluster with a bigger E_{gap} is more stable and possesses a weaker chemical activity. Figure 2(a) shows the E_{gap} of the most stable indium oxide clusters as a function of the oxygen atom ratio. The E_{gap} of all the isomers is displayed, as shown in Fig. 2(b). Due to the different structures and atomic coordinations, a trend in the energy gap is not found with the variation of oxygen atom ratio. The E_{gap} of the most stable cluster configurations varies from 0.76 eV to 4.93 eV and oscillates significantly with the oxygen ratio. Remarkable peaks are seen from In_4O_3 and InO_3 clusters to be at 4.93 eV and 3.35 eV , indicating these clusters are more stable than their neighbouring clusters. Figure 3 shows the net charge distribution of indium oxide clusters, obtained through Mulliken population analysis. The average charge residing on oxygens decreases with the

increase of oxygen/indium ratio, while an increasing trend is found for the indium atom, as expected.

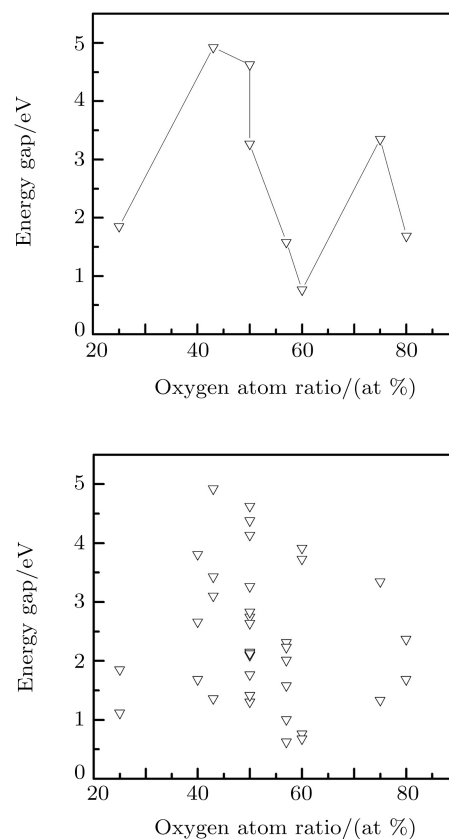


Fig. 2. The HOMO–LUMO gaps (in eV) of (a) the most stable configurations and (b) all stable configurations of indium oxide clusters.

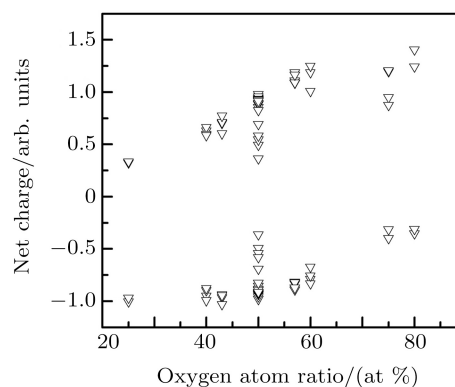


Fig. 3. Net charge distributions of all isometric configurations of indium oxide clusters.

4. Conclusions

The equilibrium structures, vibrational frequencies and electronic properties of indium oxide clusters are explored using DFT–B3LYP method with 6-31G(D) and LanL2DZ basis sets. The most stable structures prefer planar configurations with a trend to

maximize the number of ionic In–O bonds and minimize the electrostatic repulsive interaction. All these structures, but for In₂O₃ cluster, exhibit low spin electronic states. The configuration stability is further in-

vestigated by computing the vibrational frequencies. The vibrational modes are analysed and compared with the experimental results. The HOMO–LUMO gap reveals the electronic stabilities of these clusters.

References

- [1] Tanaka I, Mizuno M and Adachi H 1997 *Phys. Rev. B* **56** 3536
- [2] Fuchs F and Bechstedt F 2008 *Phys. Rev. B* **77** 155107
- [3] King P D, Veal T D, Fuchs F, Wang C Y, Payne D J, Bourlange A, Zhang H, Bell G R, Cimalla V, Ambacher O, Egdell R G, Bechstedt F and McConville C F 2009 *Phys. Rev. B* **79** 205211
- [4] Zhang D, Li C, Han S, Liu X, Tang T, Jin W and Zhou C 2003 *Appl. Phys. Lett.* **82** 112
- [5] Kim H, Piqué A, Horwitz J S, Mattoussi H, Murata H, Kafafi Z H and Chrisey D B 1999 *Appl. Phys. Lett.* **74** 3444
- [6] Kasiviswanathan S and Rangarajan G 1994 *J. Appl. Phys.* **75** 2572
- [7] Ginley D S and Bright C 2000 *MRS Bull.* **25** 15
- [8] Falcony C, Kirtley J R, Dimaria D J, Ma T P and Chen T C 1985 *J. Appl. Phys.* **58** 3556
- [9] Hamberg I and Granqvist C G 1986 *J. Appl. Phys.* **60** 123
- [10] Granqvist C G and Hultaker A 2002 *Thin Solid Films* **411** 1
- [11] Xie W 2008 *Chin. Phys. B* **17** 2683
- [12] Wang X J, Fei Y J, Xiong Y Y, Nie Y X, Feng K A and Li L D 2002 *Chin. Phys.* **11** 737
- [13] Li C, Zhang D, Liu X, Han S, Tang T, Han J and Zhou C 2003 *Appl. Phys. Lett.* **82** 1613
- [14] Zehe M J, Lynch J D, Kelsall B J and Carlson K D 1979 *J. Phys. Chem.* **83** 656
- [15] Burkholder T R, Yustein J T and Andrews L 1992 *J. Phys. Chem.* **96** 10189
- [16] Archibong E F and Sullivan R 1995 *J. Phys. Chem.* **99** 15830
- [17] Archibong E F and Sullivan R 1996 *J. Phys. Chem.* **100** 18078
- [18] Mukhopadhyay S, Gowtham S, Pandey R and Costales A 2010 *J. Mol. Struct. (THEOCHEM)* **948** 31
- [19] Becke A D 1993 *J. Chem. Phys.* **98** 5648
- [20] Lee C, Yang W and Parr R G 1988 *Phys. Rev. B* **37** 785
- [21] Frisch M J, Trucks G M, Schlegel H B, *et al.* 2003 *GAUSSIAN 03* (Pittsburg, Gaussian Inc., PA)
- [22] Gowtham S, Costales A and Pandey R 2004 *J. Phys. Chem. B* **108** 17295
- [23] Gowtham S, Deshpande M, Costales A and Pandey R 2005 *J. Phys. Chem. B* **109** 14836
- [24] Deshpande M, Kanhere D G and Pandey 2006 *J. Phys. Chem. A* **110** 3814
- [25] Gowtham S, Costales A and Pandey R 2006 *Chem. Phys. Lett.* **431** 358
- [26] Stößer G and Schnöckel H 2005 *Angew. Chem. Int. Ed.* **44** 4261
- [27] Archibong E F, Seeburrun N and Ramasami P 2009 *Chem. Phys. Lett.* **481** 169